

Journal Pre-proof

Effect of land use on microplastic pollution in a major boundary waterway: The Arvand River

Naghmeh Soltani, Behnam Keshavarzi, Farid Moore, Rosa Busquets, Mohammad Javad Nematollahi, Reza Javid, Sylvie Gobert



PII: S0048-9697(22)01821-6

DOI: <https://doi.org/10.1016/j.scitotenv.2022.154728>

Reference: STOTEN 154728

To appear in: *Science of the Total Environment*

Received date: 29 December 2021

Revised date: 25 February 2022

Accepted date: 17 March 2022

Please cite this article as: N. Soltani, B. Keshavarzi, F. Moore, et al., Effect of land use on microplastic pollution in a major boundary waterway: The Arvand River, *Science of the Total Environment* (2021), <https://doi.org/10.1016/j.scitotenv.2022.154728>

This is a PDF file of an article that has undergone enhancements after acceptance, such as the addition of a cover page and metadata, and formatting for readability, but it is not yet the definitive version of record. This version will undergo additional copyediting, typesetting and review before it is published in its final form, but we are providing this version to give early visibility of the article. Please note that, during the production process, errors may be discovered which could affect the content, and all legal disclaimers that apply to the journal pertain.

© 2022 Published by Elsevier B.V.

Effect of land use on microplastic pollution in a major boundary waterway: the Arvand River

Naghmeh Soltani^{a,*}, Behnam Keshavarzi^{a,*}, Farid Moore^a, Rosa Busquets^b, Mohammad Javad Nematollahi^a, Reza Javid^{c,d}, Sylvie Gobert^{e,f}

^a. Department of Earth Sciences, College of Science, Shiraz University, 71454 Shiraz, Iran

^b. School of Life Sciences, Pharmacy and Chemistry, Kingston University, Kingston Upon Thames, Surrey KT1 2EE, UK

^c. Khorramshahr Environmental Protection Office, Khorramshahr 6491846783, Iran

^d. Department of Marine Biology, Faculty of Marine Science and Oceanography, Khorramshahr University of Marine Science and Technology, Khorramshahr, Iran

^e. STATION de REcherche Sous-Marines et Océanographiques (STAKESO), 20260 Calvi, France

^f. Université de Liège, Centre MARE, Laboratoire d'Océanologie, Sart-Tilman, B6c, 4000 Liège, Belgium

*Corresponding authors,

Email: BKeshavarzi@shirazu.ac.ir (B. Keshavarzi)

Naghmeh.soltani@shirazu.ac.ir (N. Soltani)

Tel-Fax: +98-71-32284572

Abstract

The occurrence of microplastics (MPs) was investigated in the Arvand River (Iran). The Arvand River (200 Km) is a major water body that flows through land with diverse use and it meets the Persian Gulf. This study constitutes the first assessment of MP pollution in the Arvand river. MP monitoring has been carried out in 24 stations located along the river. The MP pollution found ranged between 1 and 291 items·L⁻¹ and 70 to 15620 items·Kg⁻¹ (dw), in water and sediment, respectively. The majority of MPs were fibres, black/gray and yellow/orange in color, and mainly 250 - 500 µm and >1000 µm in size. Polyethylene terephthalate (PET), polypropylene (PP), nylon (NYL), high-density polyethylene (HDPE), and polystyrene (PS) were found in sediment samples. All these polymers, except HDPE, were also identified in the water samples. Polyethylene terephthalate (PET) and polypropylene (PP) were dominant in the water samples; whereas PET and polystyrene (PS) were the most abundant in the sediments. The vicinity of urban wastewater effluents could be behind MP pollution in both water and sediments. Significant differences ($p < 0.05$) of MP concentrations were affected by different land uses when comparing MP levels in undisturbed natural area with urban areas. A strong correlation between MP fibers and fragments found with PCA biplots revealed their similar distribution in water. In the sediment samples, fiber and fragment MP particles were significantly correlated with colloidal particles (e.g., clay and organic matter) suggesting a relevant role of colloidal particles in the aquatic ecosystem of the Arvand River in transporting MPs. This study contributes to the better understanding of the presence of MP in major rivers, which are systems that have been scarcely investigated for this type of pollution, and it can inform interventions to reduce MP inputs to the river and sea.

Keywords: Microfibre, river, surface water, sediment, land use

Introduction

Marine plastic litter is a global challenge (Isobe et al., 2021) which directly affects marine and coastal life and ecosystems. Important amounts of plastic particles are entering aquatic ecosystems. Rivers are a major routes of plastic waste from land to the ocean. Each year, between 1.15 and 2.41 million tons of plastic waste are estimated to reach the oceans from the rivers (Lebreton et al., 2017). Riverine ecosystems are also directly affected by plastic pollution (van Emmerik and Schwarz, 2020).

Plastics can be washed from land to surface waters by direct inputs from the main sources of contamination, wind or precipitation (Duis and Coors, 2016). Elevated microplastic (MP) levels in river water and sediments can be associated with proximity to densely populated areas, industries, sewage treatment plants or tributaries (Shruti et al., 2019; Wagner et al., 2019). Sewage discharge and runoff from urban areas are indeed major contributors of plastic pollution to rivers worldwide (Streckel et al., 2021). Moreover, effluents from industries with improper treatment, and agricultural drainage strongly impact the plastic load in riverine systems (Gallagher et al., 2016; Piehl et al., 2018). The abundant plastics pollution in rivers results in negative impact on these ecosystems and their biota (Horton et al., 2017).

As plastics are designed to last, plastic waste accumulate in the marine environment for long time (Delacuvellerie et al., 2021; Wang et al., 2016). During this period, and under the influence of a number of factors such as UV irradiation, oxidants, hydrolysis and mechanical abrasion, large plastic pieces disintegrate into smaller fragments (< 5 mm) (Song et al., 2017) generally

referred to as MPs. Furthermore, some plastics directly enter the environment as primary MPs which are manufactured for a number of purposes such as personal care products, industrial abrasives (Lehtiniemi et al., 2018) or as precursors for the production of polymers.

MPs are extremely mobile in aquatic ecosystems due to their lightweight, insolubility, and durability (Holland et al., 2016). Following the entrance of MPs to surface water, they distribute in the water column (surface water and subsurface water) to superficial sediments (Hidalgo-Ruz et al., 2012; Nematollahi et al., 2020) depending on MP properties, geomorphological characteristics, water depth and velocity (Pereira et al., 2018; Sekudewicz et al., 2021).

In particular, low-density MPs can be re-suspended to surface and subsurface water, while denser MP particles remain in the lower part of the water column and become entrapped and accumulate in surface sediments (Defontaine et al., 2020; Lenaker et al., 2019). The fate of the sedimentated MP in superficial sediments will be influenced by the sediment structure, grain size (Mendes et al., 2021), its organic matter content and the bioturbation and hyporheic exchange processes (Drummond et al., 2022). Maes et al. (2017) found a positive correlation between MPs abundance and total organic carbon (TOC) of sediments. Green and Johnson (2020) observed that finer grains trap more MP particles. However, knowledge of processes affecting the fate of MPs in the river are relatively scarce (Drummond et al., 2022; Pohl et al., 2020).

MPs in both the water column and sediment can be easily mistaken for food due to small size, their olfactory trap, and hence they can be ingested or uptaken through skin and gill by a wide range of marine and freshwater organism (O'Connor et al., 2020; Savoca et al., 2016). Adverse health effects associated with the intake of MPs by marine species include physical damage, tissue abrasion and mechanical obstruction (Pozo et al., 2019). The release of plastic additives

and adsorbed toxic elements, persistent organics and substances of concern such as antibiotics and even microorganisms may occur during digestion of MPs in the digestive tracts of marine species (Caruso, 2019; Yu et al., 2021) (Delacuvellerie et al., 2022). Thus, MPs can be vectors of toxic chemicals and their intake could result in toxicity to aquatic life (Pannetier et al., 2020). Furthermore, contaminated fish and seafood can result in MPs ingested by humans and affect our health directly (Blackburn and Green, 2021). Recent studies indicates that human exposure to MPs and nanoplastics (NPs) might cause oxidative stress, cytotoxicity, neurotoxicity, reproductive toxicity, carcinogenicity, and translocation to other organs (Anbumani and Kakkar, 2018; Meng et al., 2022; Rahman et al., 2021).

The Arvand River is the most important inland water body in Iran (Zahed et al., 2008). It has been an important source of water for fisheries (local and exportation), shipping, cultivation, domestic and industrial water use and supports the ecology of the river. A variety of anthropogenic activities including residential domestic waste effluents (mainly from Abadan and Khorammshahr cities), industrial effluents (e.g., Abadan oil refinery and Abadan Petrochemical complex) and wastewater from agricultural activity surrounding the river could result in plastic pollution in the river. Thus, it is important to assess the quality of the Arvand river in term of MPs pollution. This study highlights the importance of research on MPs' distribution in water and sediment of the Arvand River under different land use (urban, industrial, agricultural and natural areas). The knowledge gained will inform pathways and fate of MP in large rivers located in areas of comparable societies.

Materials and methods

Study area

The Arvand River, also known as Shatt al-Arab in Arabic, is flowing North East the Persian Gulf, it constitutes part of the southern border between Iraq and Iran. The river watershed is situated within the Mesopotamian plain (Haghighi et al., 2020) which is covered mainly by Quaternary deposits including Holocene and Pleistocene alluvial sediments (Sissakian et al., 2017) over 100 m thick. Arvand is a wide navigable river that flows through three major cities including Basra (1,381,731 inhabitants) in Iraq, and Abadan (231,476 inhabitants) and Khorramshahr (133,097 inhabitants) in Iran (Hosseini et al., 2013). The total length of the Arvand River is 200 km (Patiris et al., 2016). Its width varies between 232 and 800 m and its depth varies between 7 and 20 m (Rahimi Moazampour et al., 2021). The river is the result of confluence of Tigris and Euphrates rivers (in Iraq), and the Karkheh and Karun rivers (in Iran). The landscape of the river is characterized by wetlands, green marshy areas, oxbow lakes, sandbars, ponds, and tidal flats (Patiris et al., 2016) which these environments support its rich biodiversity.

The hydrology of the river is governed by discharge conditions of the feeding rivers, tides from the Persian Gulf, and the effect of climatic conditions (i.e., precipitation, temperature, evaporation, and runoff) on discharge rates and solids load in the river (Allafta and Opp, 2020). The tide in the Arvand River is classified as semi-diurnal, with an average rise of 2.6 m at the mouth of the river near the Persian Gulf (Haghighi et al., 2020). In recent years, this river has experienced an increase in salinity which the total dissolved solids (TDS) value of the water exceeded 15,000 ppm, due to substantial dropping of incoming freshwater from its major feeding rivers (Hamdan, 2016).

The area where the Arvand River flows has typically hot humid summers with mild winters. According to internal report of Meteorological Department of Khuzestan Province, the annual

average precipitation of the area is 154.5 mm (year 1971-2021). The minimum and maximum temperatures are -4 and 53 °C with the annual average of 25.3 °C, respectively (year 1971-2021).

Sample collection and preparation

Surface water and sediment samples were collected considering various land uses within the river basin (i.e., urban, industrial, agricultural and natural areas). Sampling took place during two field campaigns which each one lasted five days in January 2018. 24 Sampling sites (N1 - N24) were selected along the Arvand River, over a distance of ~86 km (Fig. 1). Detailed information of sampling sites is presented in the Table S1 (Supplementary Information). Briefly, seven sites were located within the urban areas of the cities of Abadan and Khorramshahr (N1-N6, N12); four sites were near industrial units including the oil refinery and petrochemical complex in Abadan (N10, N11, N13, N14); nine sites were near agricultural farms (N7-N9, N15-N20); and four sites were natural areas (N21-N24) far from populated areas in the estuary where the river meets the Persian Gulf (Fig. 1).

At each station, 3 L water samples were collected in pre-cleaned amber glass bottles with aluminum foil-lined caps. Specifically, sample bottles were rinsed at least twice with surface water at each station and then fully submerged till the mouth of bottle was approximately 20 cm below the surface then capped immediately after filling. Undisturbed sediment samples (top 1- 5 cm) were simultaneously collected at each station within a radius of 1 m in triplicates (Fastelli et al., 2016) resulting in one bulk composite sample of 3-4 kg of wet sediment. The sediments were taken with a cleaned stainless-steel Van Veen grab sampler and were homogenised manually by stirring with a sterile spatula in a prewashed stainless-steel sheet pan, and finally placed in wide mouth amber glass jars. There were duplicates for each sampling site to reduce random errors.

All samples were transported to the laboratory and stored at 4°C until further analysis. Each composite sediment sample was split into two subsamples. The first part was stored at room temperature for 14 days in the laboratory and after complete dryness sieved through a 2-mm sieve for physico-chemical characterisation. The second part of the sample, which was used for monitoring MPs, were oven-dried at 50 °C for three days to a constant weight, weighed, and sieved through a 5-mm stainless steel sieve.

Physico-chemical parameters of sediment samples

The physico-chemical characterisation included sediment pH, electrical conductivity (EC), organic matter and cation exchange capacity (CEC). pH and EC were determined according to Ryan et al. (2001): after 10 min stirring of a 50 g dry sediment in 50 ml distilled water pH was measured using a pH-meter (Eutech instrument, Waterproof CyberScan PCD 650, Singapore). EC was determined using 1:5 water extracts (w:v) with a EC-meter (CyberScan PCD 650). Organic matter content was determined using the loss-on-ignition method (Miyazawa et al., 2000) while the hydrometer method was used for particle size distribution (Gee and Bauder, 1986). The ammonium acetate method (Kahr and Madsen, 1995) was employed to determine cation exchange capacity (CEC) in the soil.

Extraction and analysis of MPs

Water samples with recorded volume were filtered using a 2 µm pore size BOECO filter paper (grade 391, Germany) assisted with vacuum. Each filter paper was placed in a watch glass dish, covered with aluminum foil and dried in an oven for 24 h at 50 °C. The MPs in the sediment samples were purified using density separation (Dekiff et al., 2014; Nuelle et al., 2014). Briefly,

dry sediment samples (200 g) were treated with 35% (v/v) hydrogen peroxide (H_2O_2) for 21 days allowing wet peroxide oxidation to remove organic matter that impedes MP detection (Prata et al., 2019). Subsequently, the samples were vacuum filtered through BOECO filter paper and rinsed with filtered deionized water to remove remaining H_2O_2 . After, samples were brought to complete dryness on a sand bath at 60°C . Sodium iodide (NaI) solution (1.6 g/cm^3) was added and shaken for 5 min at 350 rpm and left to settle for 1.5 h. The cleared solution supernatant was centrifuged (for 5 min at 4000 rpm) and then filtered. Flotation ($n=2$) was carried out to separate MP. Supernatants were transferred to the same filter. Finally, filters were left to dry at room temperature and kept in a petri dish for further MP's visual assessment.

A binocular optical microscope with $\times 200$ magnification (Carl-Zeiss, Oberkochen/West Germany) was used to observe the filter membrane. Finally, filters were left to dry at room temperature and kept in a petri dish for further visual assessment of the particles in them. Color, size and shape of particles, identified as MP following further spectroscopic characterisation, were recorded. MP particles with characteristic dimensions of $L \leq 100 \mu\text{m}$, $100 < L \leq 250 \mu\text{m}$, $250 < L \leq 500 \mu\text{m}$, $500 < L \leq 1000 \mu\text{m}$ and $1000 < L \leq 5000 \mu\text{m}$ were considered, providing an overview of the MP's distribution. The number of MP's in water and sediment are reported as items/ m^3 and items/kg, respectively.

Surface morphology of MP's were characterized by Scanning Electron Microscope (SEM, TESCAN VEGA 3, Czech Republic) with a resolution of 2 nm with an optimized acceleration voltage of 20 kV. Qualitative elemental composition of MP's was examined by an Oxford Instruments X-Max 50 silicon drift energy-dispersive X-ray detector (EDX) with AZtec and INCA software. Previous to the analysis, MP's were placed on double-sided adhesive copper tape on aluminium SEM stubs, coated with a thin film of evaporated gold under vacuum

(Quorum Technologies Q150R ES, UK). Nonconductive MP particles require an electrically conductive surface deposition, with a thin film of a conductive material like gold to avoid charging during electron microscopy (Girão, 2020; Uheida et al., 2021). Both point and areal EDX scans were used, as appropriate (based largely on sample size), to determine the elemental composition of MP particles.

Chemical composition of MPs was determined using a high-resolution Raman spectroscopy (Lab RAM HR Evolution, HORBIA, Japan) with IR-laser with wavelength of 785 nm (max power 90 mW) laser. In addition, a special 50-percent-filter was used to control the laser power. Raman spectra were measured with a spectral resolution of 0.5 cm^{-1} in a wavenumber range of 400 to 1800 cm^{-1} using an acquisition time of 15 s accumulated every 5 scans. The device has been calibrated by recording the Raman spectrum of pure silicon wafer. HORBIA Scientific's LabSpec 6 Software was used for spectra data collection and analysis. MPs type was recognized via comparing the obtained MPs spectrums with the HORBIA Edition of the KnowItAll® standard database.

Prevention of contamination

Before sampling, tools and containers to be used were washed with deionized water pre-filtered with $2 \mu\text{m}$ BOECO filters (grade 391, Germany). Prior analysis, lab utensils and glassware were rinsed with the pre-filtered water and with ethanol. The work surfaces used for MPs extraction and counting were wiped with cotton cloth impregnated with ethanol. Cotton lab coats and clothing and nitrile gloves were the only ones worn while the MP study was ongoing. All containers used for the sampling and analysis were made of glass or stainless steel.

To minimize contamination by airborne MP particles and fibres, reagents and solutions were filtered throughout the procedure using 2 μm BOECO filters (grade 391, Germany). Laboratory blanks (consisting of material collected onto open clear glass petri dishes left near the working area during the MP purification) were analysed in parallel to water and sediment samples. A total of 3 laboratory blanks were carried out (No MPs were detected in controls).

Data analysis

Statistical tests were conducted on log-normalized data using SPSS 23 software. The independent Mann-Whitney U test and t-test were applied to compare means of MP concentrations and discriminate significant differences between water and sediment. The homogeneity of variances for the t-test was checked using Levene's statistic test. Kruskal-Wallis test was carried out to reveal significant differences ($p < 0.05$) of pH in sediment samples among the four investigated land uses.

Furthermore, to compare the means of MP concentrations between different land-uses, a one-way analysis of variance (ANOVA) was used.

To check the equality of means and verify significant differences between the means, the robust Welch and Brown-Forsythe tests based on p-values < 0.05 were employed. The Levene statistic test was used to check the homogeneity of variances and select the most efficient way to carry out one-way ANOVA. Dunnett's T3 method was used to carry out ANOVA analysis. To find interrelations between variables, the two-dimensional principal component analysis (PCA) was applied using Minitab 16, based on eigenvalues greater than 1, and the varimax rotation method. To obtain optimum component numbers and adequacy of samples, the Kaiser normalization and Kaiser-Meyer-Olkin (KMO) methods were applied, respectively. Statistical comparisons

between concentrations of MPs in sediment and water assumed that 1L of river water corresponds to 1Kg.

Results and discussion

Distribution of MPs in water and sediment

The physicochemical characteristics of the sediment samples were given in Table S2 and section S1. Microplastics were found in all surface water and sediment samples from the 24 sampling sites distributed along the Arvand River. A total of 2218 and 6195 MP items were collected from the total of 24 water and 24 sediment sampling sites, their corresponding concentration of MPs ranged from 1 to 291 items L^{-1} in water and from 70 to 15620 items kg^{-1} dw in sediment. The number of MPs in surface water was 42 times lower (Mann-Whitney U test, $p < 0.05$) than in the sediment samples when approximating that 1L of river water corresponded to 1Kg. The mean concentration of MPs in areas with contrasting land use on the river banks are illustrated in Fig. 2. Statistically significant differences were observed between the concentration of MPs in water and sediment ($p < 0.05$). Sediments could be long-term sink of MPs (Cózar et al., 2014; Ding et al., 2019; Martellini et al., 2018; Scherer et al., 2020), and they can even accumulate light microplastics with hypoxic exchange processes playing a role (Drummond et al., 2022).

Compared to other river systems, MP concentrations found in the water of the Arvand River were higher than those in the West River (2.99 to 9.87 items L^{-1}) (Huang et al., 2021) and in the Yangtze River (0.48 to 21.52 items L^{-1}) (Hu et al., 2018), both in China, and in the Vistula River in Poland (1.6 to 2.55 items L^{-1}) (Sekudewicz et al., 2021). Similarly, in sediment, MP concentrations were higher compared to levels found in the West River in China (2560 to 10240 items kg^{-1}) (Huang et al., 2021); in the Brisbane River in Australia (10 to 520 items kg^{-1}) (He et

al., 2020); in the Pearl River in China (80 to 9597 items kg^{-1}) (Lin et al., 2018), and in the Vistula River in Poland (190 to 580 items kg^{-1}) (Sekudewicz et al., 2021). Different pollution sources and levels, nearby human activities and natural factors (e.g. hydrodynamic conditions and sediments properties) have the potential to influence the distribution and abundance of MPs in aquatic ecosystems (Deng et al., 2021; Horton et al., 2017; Qian et al., 2021). The distribution of MPs in water can also be affected by the weather, the environmental conditions (Browne et al., 2011) and hyporheic exchange processes which especially affect MPs $< 100 \mu\text{m}$ (Drummond et al., 2022).

Spatial heterogeneity in MPs distribution was observed in both water and sediment samples in the study area. The MP concentrations in different land uses showed the following decreasing trend: urban $>$ industrial $>$ agricultural $>$ natural areas in surface water and sediment. The highest MPs concentrations were found in samples from the urban area representing 68% (in water) and 69% (in sediment) of all the items found, followed by industrial and agricultural land uses. In particular, site N4, which was collected near an urban wastewater discharge to the Arvand River, had the highest MP concentration in water and sediment. Wastewater effluents from Khorramshahr were discharged into the river without any treatment, and this led to levels found at site N4. These results agree with greater MP pollution in urban soils than in industrial soils in a study in Ahvaz (Iran) (Nematollahi et al., 2021). Similarly, Huang et al. (2021) showed that spatial distribution of MPs varies between different land uses, and higher MP levels were found in commercial/public/recreational areas compared to the levels in natural areas of the West River in China.

The average abundance of MPs in surface water and sediment in the study urban area was about 45 and 28 times higher than natural area in the present work. Tibbetts et al. (2018) also reported

greater MPs abundance in the sediment samples collected from the urban section of the Tame River compared with its rural section. In urban areas MPs can originate from different sources such as building sector, manufacturing industries, road litter, overflow from sewer, and vehicles traffic (Kawecki and Nowack, 2020). At industrial area, the Arvand River is impacted by receiving industrial effluents from Abadan oil refinery and Abadan petrochemical complex, which could be a major source for MPs inputs to the river. Another industrial unit in the area is Khorramshahr soap factory, where microbeads were used to manufacture soap and MPs could be discharged to the Karoon River and eventually reach the Arvand River. Although this factory has not been active for the last 10 years, MP pollution could persist in the sediment. However, significant differences were not found regarding the abundance of spherule MP particles in sampling sites near the soap factory compared to other sites.

Agricultural input is also an important source of MPs pollution at the Arvand River area. In agricultural sector of the Arvand River, application of plastic mulches in vegetable cultivation result in MPs release. Moreover, in the vicinity of Arvand River, plastics are frequently used in greenhouse farming, winter cultivation and covering small date palm trees in different stages of growth. Plastic liners are also used in ponds to increase irrigation water velocity and prevent water loss. Previous investigations have also shown that a number of farming activities contribute to MPs pollution (Cao et al., 2021; Chen et al., 2020). In natural area, fishery activities and marine transportation will affect the contamination of water and sediment with MPs (Bringer et al., 2021).

Characterization of MPs

The identified MPs in water and sediment samples varied in shape, color and size, and this diversity is illustrated in Fig. 3. In both surface water and sediment samples, fibers were the dominant MP shape in different land uses including urban (79% of water samples and 85% of sediment samples), industrial (74% of water samples and 88% of sediment samples), agricultural (80% of water samples and 88% of sediment samples) and natural (95% of water samples and 93% sediment samples). There are significant differences (Mann-Whitney, $p < 0.05$) between fiber, film, fragment and spherul particles in water and sediment samples. Higher surface to volume ratio of fiber particles, enable them to suspend in water column (Zhao et al., 2015). Fragment items were also relatively abundant in water and sediment samples compared to other MP types.

Importantly, spherules were least abundant MP in water and sediment samples (Fig. S1). Fiber was the dominant shape of MPs in water and sediment of several important rivers worldwide including Ciwalengke River in Indonesia (Alam et al., 2019), Pearl River in China (Lin et al., 2018), Haihe River in China (Liu et al., 2021), and Alaknanda River in India (Chauhan et al., 2021).

The high number of MP fibers and fragments may derive from fragmentation or weathering of discarded plastics transported over long distances by rivers (Andrady, 2017; Mani et al., 2015). The dominance of the MP particles may be attributed to the sources of pollution available in the river (Chauhan et al., 2021). Domestic washings, farm equipment, fishing nets and gear, atmospheric deposition and urban runoff, which includes debris from tyres among other types of plastics, are also potential sources of plastic fibers and fragments (Cesa et al., 2017; de Jesus Piñon-Colin et al., 2020; Dris et al., 2016). Cosmetic products and transportation packages are the main source of fragment particles (Yan et al., 2019).

Black/grey and yellow/orange were the dominant MPs colors in the surface water and sediments (Fig. S2). In general, MPs vary greatly in color depending on the parent material, but yellow/orange were the most common colors among the MPs found in the urban, industrial and agricultural sectors, while black/grey were the dominant MPs color in natural area. Different MP colors originate from various sources (Pan et al., 2019b; Xu et al., 2018). Moreover, environmental weathering especially ultraviolet oxidation (Wang et al., 2020) and MP extraction treatment (Karami et al., 2017; Nuelle et al., 2014) may cause MP.

In surface water the 250 –500 μm size fraction included higher proportion of MPs in most sampling sites. In parallel, 250 - 500 μm and $> 1000 \mu\text{m}$ MPs prevailed in the sediment samples (Fig. S3).

The enrichment of smaller-size MP particles may be that larger MP particles could gradually be split into smaller ones (Jeyasanta et al., 2020; Zhang et al., 2015). Smaller size of MP particles are prevalent in water compared to sediment samples (Mann-Whitney, $p < 0.05$). Different aquatic species can easily access to the smaller MP particles and hence MPs ingestion potentially affect them (Jeong et al., 2016).

The $> 1000 \mu\text{m}$ size is the prevalent fraction in sediment samples within urban and industrial areas. Similarly, $> 1000 \mu\text{m}$ is the most dominant size in water samples collected from urban areas. In the sediment samples of the Arvand River, larger particles ($> 1000 \mu\text{m}$) were found to be more abundant than small MPs. This can be explained by higher densities of larger particles, causing large particles to settle more quickly (Di and Wang, 2018). The distribution, fate and retention of MPs is significantly affected by the size of MP particle, regardless of the polymer type (Sagawa et al., 2018).

Morphology of MPs

SEM - EDX analyses with the elemental composition at the surface of MP are illustrated in Fig. 4. The EDX spectra of most particles exhibited a strong C signal, followed by a smaller O signal. The high percentage of C and O show that the detected MPs are organic substances that could be plastics or natural polymers. Moreover, EDX analysis of the studied MPs showed that in addition to large amounts of C and O, minor amounts of other elements such as Na, Mg, Si, Cl, and Ca, Ba, S, Fe, and I also occur as polymer additives (Fries et al., 2013, Pandey et al., 2022), adhered materials on the MP surfaces (Severini et al., 2020; Zhou et al., 2018) and MPs chemicals used in the procedure (Wagner et al., 2017) (e.g., NaI used in Mn floatation during sample treatment). Morphological features of MP surfaces with various degree of weathering were also examined by SEM analysis (Fig. 4). Compared to some fiber particles separated from water samples with relatively smooth surfaces (Fig. 4 a), most extracted MPs from sediment samples showed uneven surfaces with damaged and broken edges (Fig. 4 d, e and f). Spherule particles show weathering features as pits (Fig. 4 c). The cracks, flakes, holes and small grooves were determined in some fiber and fragments in sediment samples (Fig. S4).

The relatively rough surfaces of most MPs particles indicate that the particles probably have undergone different levels of weathering and fragmentation processes. In aquatic environments, MP particles may be affected by weathering under chemical, mechanical and biological degradation resulting in changes in MPs surface morphology (Corcoran, 2020). Wang et al. (2019) observed the morphological changes of the MPs in the Yellow Sea sediment, China including deformation and fracture indicating that MPs would crack into smaller pieces.

The surface roughness and cracks probably generate during particle transportation and prolonged residence in aquatic environment (Pan et al., 2019a) but some could be generated during the SEM imaging of the sample.

Weathering of MPs can be determined by cracks, pits and flakes and adhering materials (Wang et al., 2017) which affect their sorption capacity towards other materials such as organic and inorganic chemicals (Dong et al., 2020). Liu et al. (2019) concluded that the MPs with smooth surfaces have weak adhesion ability, while those with rough surface have stronger adhesion ability. Cai et al. (2018) used SEM images to demonstrate that the surfaces of the pristine MPs become rougher under UV irradiation and it makes plastic susceptible to fragmentation (Wang et al., 2021).

The EDX results of two weathered particle revealed a decrease in C (W%) in the weathered MP particles with rough surfaces (Fig. S4 a, b) compared to the pristine MPs with smooth surfaces (Fig. 4 a, b, and e). During weathering processes physicochemical properties of MPs (e.g. color, size, structure, mechanical characteristic and oxygen functional groups) may result in release of toxic additives and absorbed chemicals (Liu et al., 2020).

The toxic leachates from weathered MPs cause potential adverse effects on organisms (Campanale et al., 2020, Simon et al., 2021). Using SEM/EDX, Fries et al. (2013) showed that the presence of Al and Zn could be related to the ability of MP particles to attract these elements while titanium-dioxide nanoparticles (TiO₂-NPs) could leach from polymer from its use as additive. MPs have different resistance to weathering, depending on their properties and polymer additives (Andrady, 2017).

Polymer composition

Raman spectroscopy is widely used to characterize MPs due to their non-destructible and rich spectrum (Araujo et al., 2018). Raman spectroscopy was used for the determination of the MP polymer composition. Fig. 5 shows the spectra of isolated MPs from the sediment and water samples. Overall, five polymers including polyethylene terephthalate (PET), polypropylene (PP), nylon (NYL), high-density polyethylene (HDPE), and polystyrene (PS) were detected in sediment samples. The same polymers except for HDPE were also detected in water samples. PET (25%), PS (22%) and HDPE (18%) were the prevalent polymers in sediment samples, while most MP particles in the water samples were made of PP (31%) and PET (24%).

Most fiber particles in the water samples were identified as NYL (33%) followed by PET (27%). Similarly, fragment MPs comprised mainly PP, accounting for 36% of the total fragment MPs. In the sediment samples, fibers were mostly made of PET (34%) and PS (23%) and fragments were made of HDPE (35%). In the water samples, PET had the largest share of MPs (39%) in urban area, followed by PS comprising 31% of the detected polymer (Fig. 6 and Table S3). In industrial sites, PET (44%) was detected as a dominant type of MP. PP was the dominant polymer type in agricultural and natural areas with percentages of 42 and 75%, respectively. In sediment samples, PET was the dominant polymer in the urban (37%) area, while HDPE (39%) was the prevalent polymer in industrial sectors. PS, PP and HDPE were major polymer types in sediment in agricultural sites. Similar to water samples, PP (56%) was the dominant polymer in natural area of the river.

The composition of MPs found in this study included PET, PP, PS, NYL, and HDPE, which also represent the most commonly encountered polymers in the aquatic ecosystem (Andrady, 2011). The proportion of high-density polymers including PET, PS and NYL appeared higher but not significantly ($p > 0.05$) in the sediment samples (66%) compared to the water samples (33%).

The results show that PP (31%) is the most common polymer in the water samples, while PET (25%) and PS (22%) are the most abundant polymers in the sediment samples. Due to lower density, PP (density: 0.895 – 0.92 g/cm³) is found suspended in the surface water (Erni-Cassola et al., 2019; Issac and Kandasubramanian, 2021).

PET with the density of 1.38 – 1.41 g/cm³ is classified as dense MPs and hence prone to settle after entering the marine environment (Driedger et al., 2015). Denser MPs such as PET, NYL and PS, with density ranging from 1.04 to 1.41 g/cm³, were identified in water samples while lightweight MPs including PP was extracted from sediment samples. The presence of light density particles in sediment can be explained by several processes that increase MP density and increase its hydrophobic nature including weathering, biofouling, hetero-aggregation or biomolecule adsorption that enhances deposition of MPs in to the sediments (Chubarenko et al., 2016; Kaiser et al., 2017). Adsorption or incorporation of foreign substances such as clay minerals or quartz grains in surficial pores and cracks of weathered MPs may change sinking behavior of MPs (Dai et al., 2018; Zhou et al., 2018). In this study, adhered mineral deposits were found onto particles. This is illustrated with the EDX compositions from deposits onto fragments and fibres shown in Fig. S4. Conversely, resuspension of bottom sediments result in re-entrance of denser MP into the water column (Lambert and Wagner, 2018).

The identification of chemical composition of the MPs may reveal the origin of the released MPs (Pan et al., 2019a). The results showed that different polymer types probably were released from different land uses. For instance, PET and PS were the main type of polymers in surface water and sediment of the urban sites. PET is commonly used in household cleaning products, clothing industry, cable lining, plastic beverage containers, and packaging (Gong et al., 2018; Guerranti et al., 2019).

PS is a thermoplastic polymer with a wide variety of applications such as packaging, household appliances, medical items, construction, and electronics (Lynwood, 2014). The predominant HDPE MPs observed in sediment samples collected near industrial units may originate from industrial effluent mostly from Abadan oil refinery and Abadan petrochemical complex. Wastewater from industries with improper treatment is also a main relevant plastic source (Gallagher et al., 2016).

HDPE, a commonly used polymer, is resistant to a broad range of chemicals (Osborne, 2008) and has variable applications in pipe systems, bulk containers for industrial use, cables and wires cover, processing equipment, industrial chemicals such as detergents, bleach and acids (Peacock, 2000; Sam et al., 2014). The predominance of PS, PP and HDPE was observed in water and sediment of agricultural areas. Different types of MPs are released from agricultural soils into water bodies as a result of applying sewage sludge and compost for soil amendment and also plasticulture in agricultural practices (Rochman, 2018; Yang et al., 2021). Ding et al. (2020) also reported PS and PP in agricultural soil of Shaanxi Province, China. Similarly, Corradini et al. (2021) observed that PS and PP were predominant polymers in crop lands (Chile).

Agricultural HDPE pipes are generally used to transport chemical fertilizers through irrigation water to the farmlands (Caj and Madramootoo, 2021). PP was the most abundant MPs in water and sediment of natural area where fishing is a common practice in this area due to proximity to the Persian Gulf. Thus, PP used in fishing ropes and nets are probably the main source of MP pollution. Jang et al. (2020) also found higher proportion of PP from the rural site of Geoje, South Korea and related it to the widespread use of PP rope in fishing.

Interrelations of MP concentrations in the environment

Interrelations of MP concentrations between water and sediment indicated significant differences between the two media ($p < 0.05$) (Table 1). This can result from a range of factors governing MP distribution in water and sediment, suggesting that MP distribution in each medium should be evaluated separately. Furthermore, physicochemical properties of sediments are seemingly important parameters in controlling MP distribution. The mean MP concentrations in each land use indicated significant differences between MP concentrations in the undisturbed natural environment and other areas in both water and sediment ($p < \text{or close to } 0.05$), despite the fact that there is no significant co-relationship between MP concentrations in other land uses ($p > 0.05$). This implies that urban, industrial and agricultural sectors constitute major sources of MPs pollution towards the Arvand River.

PCA biplots, including two principal components (PCs), revealed the interrelations between types of MPs, sediment parameters, sampling sites and land uses in both media (Fig. 7). In water, PC1 and PC2, accounted for 68 and 17 % of total variances, respectively (Fig. 7 a). PC1 was greatly responsible for MP distribution in water and MP fibers and fragments fell in PC1 and had a strong correlation, indicating that they comply with similar distribution in the water sampling sites. Scores of water samples in the PCA indicated that N4 (sampling site near an urban wastewater effluent) had a very strong positive score in both PCs, reflecting that N4 greatly controls the distribution of different types of MPs. However, positive sample scores of N4, N12, N5, N14, N16, N17, N13, N11, and N7 in PC1 are can be affected by the distribution of fibers and fragments in water. The distribution of MP films and spherules is mainly governed by positive scores of N4, N7, and N10, and N4 in PC2, respectively. The PCA revealed that the highest and lowest concentration of MPs emitted into the water from urban and natural land uses, respectively.

In sediment, PC1 and PC2 explained 33 and 26 % of total variances and MPs contributed to both PCs. Fiber, fragment and clay, had greater influence in PC1; and film, spherule and OM carbonate in PC2 were co-correlated and have high positive factor loadings, respectively. Sand was inversely correlated with the MPs and it could indicate that it is related with low levels of them due to the effect of sand filtration. N4 had the highest sample score in PC1 (Fig. 7 b) followed by N5, N3, N16, N12, N17, N2, N14, N15, N19, and N13, respectively, while in PC2, the highest sample scores were N11, N9, N17, N7, N12, N10, N6, N13, N5 and N14.

Based on sample scores, the degree of contamination (PC1) was mainly affected by the fiber and fragment release from urban sources and are associated with or controlled by clay and OM, whereas film and spherule MPs (PC2) are mainly influenced by industrial and agricultural land uses and are mostly associated with carbonate and sand in sediment. Similar to water, natural land use released the lowest concentration of MPs into the sediment.

Sample score of sediment implied that clay and OM are good explanatory factors in distributing fibers and fragments, while carbonate and sand are factors that well explain the distribution of MP film and spherule in sediment. Recent studies have indicated the interaction of OM and clay fraction with MPs by attaching to MP particles and influencing their fate and transport in aquatic environments (Li et al., 2021). The stability and migration capability of MPs is influenced by humic and fulvic acid attached to MPs (Dong et al., 2019; Hou et al., 2020). Maes et al. (2017) found a positive correlation between concentration of MPs and total organic carbon (TOC) in sediment of the Southern North Sea. Green and Johnson (2020) observed that finer sediments with high TOC, trap more MPs than sediments with low TOC.

The transport of MPs can be affected by clay minerals such as kaolinite that adsorb onto MP surfaces (Li et al., 2020). Enders et al. (2019) found a significant correlation between fine

sediment fraction ($<63 \mu\text{m}$) of sediment and MPs in the Warnow estuary in Germany. Elevated MP particles separated from fine-grained sediments are probably the result of higher surface tension of fine-grained particles (Stolte et al., 2015). In this study, a large number of MP particles, fibers and fragments, indicated good correlations with colloidal particles, clay and OM, reflecting that the colloidal particles in aquatic ecosystem of Arvand River may have played a crucial role in transport and fate of MPs.

Conclusion

This study is the first research work that examines the occurrence and characteristics of MPs in urban, industrial, agricultural and natural areas of the Arvand River and it leads to better insights into the source and distribution of MPs in a large river system. Larger MPs were more prevalent in sediments and this compartment can act as a major sink for MP debris. There was positive correlation between MP concentrations and colloidal particles including clay and OM. This points towards a potential role of OM hydrophilicity and particle size of natural matter on the transport and ultimate fate of MPs.

The decreasing order of the average abundance of MPs in water and sediment was urban > industrial > agricultural > and natural areas ($p > 0.05$). Natural areas of the Arvand River are still relatively pristine in term of MP pollution. In contrast, no statistically significant differences of MPs distribution were found among urban, industrial and agricultural sources and this indicate that they are all potential sources or pathways of MPs pollution. The Arvand River is highly affected by human activity with regards to plastic pollution and thus corrective actions should be taken by scientific community, the industry, policy-makers and civil society to minimize the

continuous flux of plastics into the environment. The results of this research will support future MP pollution monitoring in water and sediment in the Arvand River and other grand rivers.

Acknowledgment

The current study was logistically supported by Shiraz University Medical Geology Center and Shiraz University Research Committee. The authors also appreciate the support of Khorramshahr Environmental Protection Office for their assistance with sample collection.

Reference

- Alam, F.C., Sembiring, E., Muntalif, B.S., Suendo, V., 2019. Microplastic distribution in surface water and sediment river around slum and industrial area (case study: Ciwalengke River, Majalaya district, Indonesia). *Chemosphere* 224, 637–645.
- Allafta, H., Opp, C., 2020. Spatio-temporal variability and pollution sources identification of the surface sediments of Shatt Al-Arab River, Southern Iraq. *Sci. Rep.* 10, 1–16.
- Anbumani, S., Kakkar, P., 2018. Ecotoxicological effects of microplastics on biota: a review. *Environ. Sci. Pollut. Res.* 25, 14373–14396.
- Andrady, A.L., 2017. The plastic in microplastics: A review. *Mar. Pollut. Bull.* 119, 12–22.
- Andrady, A.L., 2011. Microplastics in the marine environment. *Mar. Pollut. Bull.* 62, 1596–1605.
- Araujo, C.F., Nolasco, M.M., Ribeiro, A.M.P., Ribeiro-Claro, P.J.A., 2018. Identification of microplastics using Raman spectroscopy: Latest developments and future prospects. *Water Res.* 142, 426–440.
- Blackburn, K., Green, D., 2021. The potential effects of microplastics on human health: What is

known and what is unknown. *Ambio* 1–13.

Bringer, A., Le Floch, S., Kerstan, A., Thomas, H., 2021. Coastal ecosystem inventory with characterization and identification of plastic contamination and additives from aquaculture materials. *Mar. Pollut. Bull.* 167, 112286.

Browne, M.A., Crump, P., Niven, S.J., Teuten, E., Tonkin, A., Galloway, T., Thompson, R., 2011. Accumulation of microplastic on shorelines worldwide: sources and sinks. *Environ. Sci. Technol.* 45, 9175–9179.

Cai, L., Wang, J., Peng, J., Wu, Z., Tan, X., 2018. Observation of the degradation of three types of plastic pellets exposed to UV irradiation in three different environments. *Sci. Total Environ.* 628, 740–747.

Campanale, C., Massarelli, C., Savino, I., Locaputo, V., Uricchio, V.F., 2020. A detailed review study on potential effects of microplastics and additives of concern on human health. *Int. J. Environ. Res. Public Health* 17, 1212.

Cao, L., Wu, D., Liu, P., Hu, W., Xu, L., Sun, Y., Wu, Q., Tian, K., Huang, B., Yoon, S.J., 2021. Occurrence, distribution and affecting factors of microplastics in agricultural soils along the lower reaches of Yangtze River, China. *Sci. Total Environ.* 794, 148694.

Caruso, G., 2019. Microplastics as vectors of contaminants. *Mar. Pollut. Bull.* 146, 921–924.

Cesa, F.S., Turra, A., Baroque-Ramos, J., 2017. Synthetic fibers as microplastics in the marine environment: a review from textile perspective with a focus on domestic washings. *Sci. Total Environ.* 598, 1116–1129.

Chauhan, J.S., Semwal, D., Nainwal, M., Badola, N., Thapliyal, P., 2021. Investigation of microplastic pollution in river Alaknanda stretch of Uttarakhand. *Environ. Dev. Sustain.* 23, 16819–16833.

- Chen, G., Fu, Z., Yang, H., Wang, J., 2020. An overview of analytical methods for detecting microplastics in the atmosphere. *TrAC Trends Anal. Chem.* 115981.
- Chubarenko, I., Bagaev, A., Zobkov, M., Esiukova, E., 2016. On some physical and dynamical properties of microplastic particles in marine environment. *Mar. Pollut. Bull.* 108, 105–112.
- Corcoran, P.L., 2020. Degradation of Microplastics in the Environment. *Handb. Microplastics Environ.* 1–12.
- Corradini, F., Casado, F., Leiva, V., Huerta-Lwanga, E., Geissen, V., 2021. Microplastics occurrence and frequency in soils under different land uses on a regional scale. *Sci. Total Environ.* 752, 141917.
- Cózar, A., Echevarría, F., González-Gordillo, J.I., Irigoien, X., Úbeda, B., Hernández-León, S., Palma, Á.T., Navarro, S., García-de-Lomas, J., Ruiz, A., 2014. Plastic debris in the open ocean. *Proc. Natl. Acad. Sci.* 111, 10239–10244.
- Dai, Z., Zhang, H., Zhou, Q., Tian, Y., Chen, T., Tu, C., Fu, C., Luo, Y., 2018. Occurrence of microplastics in the water column and sediment in an inland sea affected by intensive anthropogenic activities. *Environ. Pollut.* 242, 1557–1565.
- de Jesus Piñon-Colin, T., Rodríguez-Jimenez, R., Rogel-Hernandez, E., Alvarez-Andrade, A., Wakida, F.T., 2020. Microplastics in stormwater runoff in a semiarid region, Tijuana, Mexico. *Sci. Total Environ.* 704, 135411.
- Defontaine, S., Sous, D., Tesan, J., Monperrus, M., Lenoble, V., Lanceleur, L., 2020. Microplastics in a salt-wedge estuary: Vertical structure and tidal dynamics. *Mar. Pollut. Bull.* 160, 111688.
- Dekiff, J.H., Remy, D., Klasmeier, J., Fries, E., 2014. Occurrence and spatial distribution of microplastics in sediments from Norderney. *Environ. Pollut.* 186, 248–256.

- Delacuvellerie, A., Benali, S., Cyriaque, V., Moins, S., Raquez, J.-M., Gobert, S., Wattiez, R., 2021. Microbial biofilm composition and polymer degradation of compostable and non-compostable plastics immersed in the marine environment. *J. Hazard. Mater.* 419, 126526.
- Delacuvellerie, A., Géron, A., Gobert, S., Wattiez, R., 2022. New insights into the functioning and structure of the PE and PP plastispheres from the Mediterranean Sea. *Environ. Pollut.* 118678.
- Deng, H., He, J., Feng, D., Zhao, Y., Sun, W., Yu, H., Ge, C., 2021. Microplastics pollution in mangrove ecosystems: a critical review of current knowledge and future directions. *Sci. Total Environ.* 753, 142041.
- Di, M., Wang, J., 2018. Microplastics in surface water and sediments of the Three Gorges Reservoir, China. *Sci. Total Environ.* 616, 627–627.
- Ding, L., fan Mao, R., Guo, X., Yang, X., Zhang, Q., Yang, C., 2019. Microplastics in surface waters and sediments of the Wei River, in the northwest of China. *Sci. Total Environ.* 667, 427–434.
- Ding, L., Zhang, S., Wang, X., Yang, X., Zhang, C., Qi, Y., Guo, X., 2020. The occurrence and distribution characteristics of microplastics in the agricultural soils of Shaanxi Province, in north-western China. *Sci. Total Environ.* 720, 137525.
- Dong, M., Luo, Z., Jiang, Q., Xing, X., Zhang, Q., Sun, Y., 2020. The rapid increases in microplastics in urban lake sediments. *Sci. Rep.* 10, 1–10.
- Dong, Z., Zhu, L., Zhang, W., Huang, R., Lv, X., Jing, X., Yang, Z., Wang, J., Qiu, Y., 2019. Role of surface functionalities of nanoplastics on their transport in seawater-saturated sea sand. *Environ. Pollut.* 255, 113177.
- Driedger, A.G.J., Dürr, H.H., Mitchell, K., Van Cappellen, P., 2015. Plastic debris in the

- Laurentian Great Lakes: a review. *J. Great Lakes Res.* 41, 9–19.
- Dris, R., Gasperi, J., Saad, M., Mirande, C., Tassin, B., 2016. Synthetic fibers in atmospheric fallout: a source of microplastics in the environment? *Mar. Pollut. Bull.* 104, 290–293.
- Drummond, J.D., Schneidewind, U., Li, A., Hoellein, T.J., Krause, S., Packman, A.I., 2022. Microplastic accumulation in riverbed sediment via hyporheic exchange from headwaters to mainstems. *Sci. Adv.* 8, eabi9305.
- Duis, K., Coors, A., 2016. Microplastics in the aquatic and terrestrial environment: sources (with a specific focus on personal care products), fate and effects. *Environ. Sci. Eur.* 28, 1–25.
- Enders, K., Käßler, A., Biniash, O., Feldens, P., Stellberg, N., Lange, X., Fischer, D., Eichhorn, K.-J., Pollehne, F., Oberbeckmann, S., 2019. Tracing microplastics in aquatic environments based on sediment analogies. *Sci. Rep.* 9, 1–15.
- Erni-Cassola, G., Zadjelovic, V., Gibson, M.J., Christie-Oleza, J.A., 2019. Distribution of plastic polymer types in the marine environment; A meta-analysis. *J. Hazard. Mater.* 369, 691–698.
- Fastelli, P., Blašković, A., Bernardi, G., Romeo, T., Čížmek, H., Andaloro, F., Russo, G.F., Guerranti, C., Renzi, M., 2016. Plastic litter in sediments from a marine area likely to become protected (Aeolian Archipelago's islands, Tyrrhenian sea). *Mar. Pollut. Bull.* 113, 526–529.
- Fries, E., Dekiff, J.H., Willmeyer, J., Nuelle, M.-T., Ebert, M., Remy, D., 2013. Identification of polymer types and additives in marine microplastic particles using pyrolysis-GC/MS and scanning electron microscopy. *Environ. Sci. Process. impacts* 15, 1949–1956.
- Gaj, N., Madramootoo, C.A., 2021. Structural response of non-perforated and perforated corrugated high-density polyethylene pipes under variable loading. *Biosyst. Eng.* 207, 120–140.

- Gallagher, A., Rees, A., Rowe, R., Stevens, J., Wright, P., 2016. Microplastics in the Solent estuarine complex, UK: an initial assessment. *Mar. Pollut. Bull.* 102, 243–249.
- Gee, G., Bauder, J., 1986. Particle-size analysis. In ‘Methods of soil analysis. Part 1. Physical and mineralogical methods’. (Ed. A Klute) pp. 383–411. Soil Sci. Soc. Am. Madison, WI.
- Girão, A.V., 2020. SEM/EDS and Optical Microscopy Analysis of Microplastics. *Handb. Microplastics Environ.* 1–22.
- Gong, J., Kong, T., Li, Y., Li, Q., Li, Z., Zhang, J., 2018. Biodegradation of microplastic derived from poly (ethylene terephthalate) with bacterial whole-cell biocatalysts. *Polymers (Basel)* 10, 1326.
- Green, B.C., Johnson, C.L.E., 2020. Characterisation of microplastic contamination in sediment of England’s inshore waters. *Mar. Pollut. Bull.* 151, 110788.
- Guerranti, C., Martellini, T., Perra, G., Scopetani, C., Cincinelli, A., 2019. Microplastics in cosmetics: Environmental issues and needs for global bans. *Environ. Toxicol. Pharmacol.* 68, 75–79.
- Haghighi, A.T., Sadegh, M., Bhattacharjee, J., Sönmez, M.E., Noury, M., Yilmaz, N., Noori, R., Kløve, B., 2020. The impact of river regulation in the Tigris and Euphrates on the Arvandroud Estuary. *Prog. Phys. Geogr. Earth Environ.* 44, 948–970.
- Hamdan, A.N., 2016. Simulation of salinity intrusion from Arabian Gulf to Shatt Al-Arab River. *Basrah J. Eng. Sci.* 16, 28–32.
- He, B., Goonetilleke, A., Ayoko, G.A., Rintoul, L., 2020. Abundance, distribution patterns, and identification of microplastics in Brisbane River sediments, Australia. *Sci. Total Environ.* 700, 134467.
- Hidalgo-Ruz, V., Gutow, L., Thompson, R.C., Thiel, M., 2012. Microplastics in the marine

- environment: a review of the methods used for identification and quantification. *Environ. Sci. Technol.* 46, 3060–3075.
- Holland, E.R., Mallory, M.L., Shutler, D., 2016. Plastics and other anthropogenic debris in freshwater birds from Canada. *Sci. Total Environ.* 571, 251–258.
- Horton, A.A., Walton, A., Spurgeon, D.J., Lahive, E., Svendsen, C., 2017. Microplastics in freshwater and terrestrial environments: evaluating the current understanding to identify the knowledge gaps and future research priorities. *Sci. Total Environ.* 586, 127–141.
- Hosseini, M., Nabavi, S.M.B., Parsa, Y., 2013. Bioaccumulation of trace mercury in trophic levels of benthic, benthopelagic, pelagic fish species, and sea birds from Arvand River, Iran. *Biol. Trace Elem. Res.* 156, 175–180.
- Hou, J., Xu, X., Lan, L., Miao, L., Xu, Y., You, C., Jiu, Z., 2020. Transport behavior of micro polyethylene particles in saturated quartz sand: Impacts of input concentration and physicochemical factors. *Environ. Pollut.* 263, 114499.
- Hu, L., Chernick, M., Hinton, D.E., Shi, H., 2018. Microplastics in small waterbodies and tadpoles from Yangtze River Delta, China. *Environ. Sci. Technol.* 52, 8885–8893.
- Huang, D., Li, X., Ouyang, Z., Zhao, X., Wu, R., Zhang, C., Lin, C., Li, Y., Guo, X., 2021. The occurrence and abundance of microplastics in surface water and sediment of the West River downstream, in the south of China. *Sci. Total Environ.* 756, 143857.
- Isobe, A., Azuma, T., Cordova, M.R., Cózar, A., Galgani, F., Hagita, R., Kanhai, L.D., Imai, K., Iwasaki, S., Kako, S., 2021. A multilevel dataset of microplastic abundance in the world's upper ocean and the Laurentian Great Lakes. *Microplastics and Nanoplastics* 1, 1–14.
- Issac, M.N., Kandasubramanian, B., 2021. Effect of microplastics in water and aquatic systems. *Environ. Sci. Pollut. Res.* 1–19.

- Jang, M., Shim, W.J., Cho, Y., Han, G.M., Song, Y.K., Hong, S.H., 2020. A close relationship between microplastic contamination and coastal area use pattern. *Water Res.* 171, 115400.
- Jeong, C.-B., Won, E.-J., Kang, H.-M., Lee, M.-C., Hwang, D.-S., Hwang, U.-K., Zhou, B., Souissi, S., Lee, S.-J., Lee, J.-S., 2016. Microplastic size-dependent toxicity, oxidative stress induction, and p-JNK and p-p38 activation in the monogonont rotifer (*Brachionus koreanus*). *Environ. Sci. Technol.* 50, 8849–8857.
- Jeyasanta, K.I., Patterson, J., Grimsditch, G., Edward, J.K.P., 2020. Occurrence and characteristics of microplastics in the coral reef, sea grass and near shore habitats of Rameswaram Island, India. *Mar. Pollut. Bull.* 160, 111574.
- Kahr, G., Madsen, F.T., 1995. Determination of the cation exchange capacity and the surface area of bentonite, illite and kaolinite by methylene blue adsorption. *Appl. Clay Sci.* 9, 327–336.
- Kaiser, D., Kowalski, N., Waniek, J.J., 2017. Effects of biofouling on the sinking behavior of microplastics. *Environ. Res. Lett.* 12, 124003.
- Karami, A., Golieskardi, A., Cho, C.K., Romano, N., Ho, Y. Bin, Salamatnia, B., 2017. A high-performance protocol for extraction of microplastics in fish. *Sci. Total Environ.* 578, 485–494.
- Kawecki, D., Nowack, B., 2020. A proxy-based approach to predict spatially resolved emissions of macro-and microplastic to the environment. *Sci. Total Environ.* 748, 141137.
- Lambert, S., Wagner, M., 2018. Microplastics are contaminants of emerging concern in freshwater environments: an overview. *Freshw. microplastics* 1–23.
- Lebreton, L.C.M., Van Der Zwet, J., Damsteeg, J.-W., Slat, B., Andrady, A., Reisser, J., 2017. River plastic emissions to the world's oceans. *Nat. Commun.* 8, 1–10.

- Lehtiniemi, M., Hartikainen, S., Näkki, P., Engström-Öst, J., Koistinen, A., Setälä, O., 2018. Size matters more than shape: Ingestion of primary and secondary microplastics by small predators. *Food webs* 17, e00097.
- Lenaker, P.L., Baldwin, A.K., Corsi, S.R., Mason, S.A., Reneau, P.C., Scott, J.W., 2019. Vertical distribution of microplastics in the water column and surficial sediment from the Milwaukee River Basin to Lake Michigan. *Environ. Sci. Technol.* 53, 12227–12237.
- Li, M., He, L., Zhang, X., Rong, H., Tong, M., 2020. Different surface charged plastic particles have different cotransport behaviors with kaolinite particles in porous media. *Environ. Pollut.* 267, 115534.
- Li, M., Zhang, X., Yi, K., He, L., Han, P., Tong, M., 2021. Transport and deposition of microplastic particles in saturated porous media: Co-effects of clay particles and natural organic matter. *Environ. Pollut.* 117505.
- Lin, L., Zuo, L.-Z., Peng, J.-P., Cai, L. Q., Fok, L., Yan, Y., Li, H.-X., Xu, X.-R., 2018. Occurrence and distribution of microplastics in an urban river: a case study in the Pearl River along Guangzhou City, China. *Sci. Total Environ.* 644, 375–381.
- Liu, P., Zhan, X., Wu, X., Li, J., Wang, H., Gao, S., 2020. Effect of weathering on environmental behavior of microplastics: Properties, sorption and potential risks. *Chemosphere* 242, 125193.
- Liu, S., Jian, M., Zhou, L., Li, W., 2019. Distribution and characteristics of microplastics in the sediments of Poyang Lake, China. *Water Sci. Technol.* 79, 1868–1877.
- Liu, Y., You, J., Li, Y., Zhang, J., He, Y., Breider, F., Tao, S., Liu, W., 2021. Insights into the horizontal and vertical profiles of microplastics in a river emptying into the sea affected by intensive anthropogenic activities in Northern China. *Sci. Total Environ.* 779, 146589.

- Lynwood, C., 2014. Polystyrene: synthesis, characteristics, and applications. Nova Publishers.
- Maes, T., Van der Meulen, M.D., Devriese, L.I., Leslie, H.A., Huvet, A., Frère, L., Robbens, J., Vethaak, A.D., 2017. Microplastics baseline surveys at the water surface and in sediments of the North-East Atlantic. *Front. Mar. Sci.* 4, 135.
- Mani, T., Hauk, A., Walter, U., Burkhardt-Holm, P., 2015. Microplastics profile along the Rhine River. *Sci. Rep.* 5, 1–7.
- Martellini, T., Guerranti, C., Scopetani, C., Ugolini, A., Chelazzi, D., Cincinelli, A., 2018. A snapshot of microplastics in the coastal areas of the Mediterranean Sea. *TrAC Trends Anal. Chem.* 109, 173–179.
- Mendes, A.M., Golden, N., Bermejo, R., Morrison, J., 2021. Distribution and abundance of microplastics in coastal sediments depends on grain size and distance from sources. *Mar. Pollut. Bull.* 172, 112802.
- Meng, X., Zhang, J., Wang, W., Gonzalez-Gil, G., Vrouwenvelder, J.S., Li, Z., 2022. Effects of nano-and microplastics on kidney: Physicochemical properties, bioaccumulation, oxidative stress and immunoreaction. *Chemosphere* 288, 132631.
- Miyazawa, M., Pavan, M.A., De Oliveira, E.L., Ionashiro, M., Silva, A.K., 2000. Gravimetric determination of soil organic matter. *Brazilian Arch. Biol. Technol.* 43, 475–478.
- Nematollahi, M.J., Keshavarzi, B., Mohit, F., Moore, F., Busquets, R., 2021. Microplastic occurrence in urban and industrial soils of Ahvaz metropolis: A city with a sustained record of air pollution. *Sci. Total Environ.* 152051.
- Nematollahi, M.J., Moore, F., Keshavarzi, B., Vogt, R.D., Saravi, H.N., Busquets, R., 2020. Microplastic particles in sediments and waters, south of Caspian Sea: Frequency, distribution, characteristics, and chemical composition. *Ecotoxicol. Environ. Saf.* 206,

111137.

- Nuelle, M.-T., Dekiff, J.H., Remy, D., Fries, E., 2014. A new analytical approach for monitoring microplastics in marine sediments. *Environ. Pollut.* 184, 161–169.
- O'Connor, J.D., Murphy, S., Lally, H.T., O'Connor, I., Nash, R., O'Sullivan, J., Bruen, M., Heerey, L., Koelmans, A.A., Cullagh, A., 2020. Microplastics in brown trout (*Salmo trutta* Linnaeus, 1758) from an Irish riverine system. *Environ. Pollut.* 267, 115572.
- Osborne, C., 2008. Hdpe Solves Alkylation Sewer Corrosion Problem In Refinery, in: *CORROSION 2008*. OnePetro.
- Pan, Z., Guo, H., Chen, H., Wang, S., Sun, X., Zou, Q., Zhang, Y., Lin, H., Cai, S., Huang, J., 2019a. Microplastics in the Northwestern Pacific: Abundance, distribution, and characteristics. *Sci. Total Environ.* 650, 1913–1922.
- Pan, Z., Liu, Q., Sun, Y., Sun, X., Lin, H., 2019b. Environmental implications of microplastic pollution in the Northwestern Pacific Ocean. *Mar. Pollut. Bull.* 146, 215–224.
- Pandey, D., Banerjee, T., Badola, N., Chauhan, J.S., 2022. Evidences of Microplastic in Air and Street Dust: A Case Study of Varanasi City, India.
- Pannetier, P., Morin, B., Leblond, F., Dubreil, L., Clérandeau, C., Chouvellon, F., Van Arkel, K., Danion, M., Cachot, J., 2020. Environmental samples of microplastics induce significant toxic effects in fish larvae. *Environ. Int.* 134, 105047.
- Patiris, D.L., Tsabaris, C., Anagnostou, C.L., Androulakaki, E.G., Pappa, F.K., Eleftheriou, G., Sgouros, G., 2016. Activity concentration and spatial distribution of radionuclides in marine sediments close to the estuary of Shatt al-Arab/Arvand Rud River, the Gulf. *J. Environ. Radioact.* 157, 1–15.
- Peacock, A., 2000. *Handbook of polyethylene: structures: properties, and applications*. CRC

press.

- Piehl, S., Leibner, A., Löder, M.G.J., Dris, R., Bogner, C., Laforsch, C., 2018. Identification and quantification of macro-and microplastics on an agricultural farmland. *Sci. Rep.* 8, 1–9.
- Pohl, F., Eggenhuisen, J.T., Kane, I.A., Clare, M.A., 2020. Transport and burial of microplastics in deep-marine sediments by turbidity currents. *Environ. Sci. Technol.* 54, 4180–4189.
- Pozo, K., Gomez, V., Torres, M., Vera, L., Nuñez, D., Oyarzún, P., Mendoza, G., Clarke, B., Fossi, M.C., Bains, M., 2019. Presence and characterization of microplastics in fish of commercial importance from the Biobío region in central Chile. *Mar. Pollut. Bull.* 140, 315–319.
- Prata, J.C., da Costa, J.P., Girão, A. V, Lopes, I., Duarte, A.C., Rocha-Santos, T., 2019. Identifying a quick and efficient method of removing organic matter without damaging microplastic samples. *Sci. Total Environ.* 686, 131–139.
- Qian, J., Tang, S., Wang, P., Lu, B., Li, K., Jin, W., He, X., 2021. From source to sink: Review and prospects of microplastics in wetland ecosystems. *Sci. Total Environ.* 758, 143633.
- Rahimi Moazampour, S., Nabavi, S.M.B., Mohammadi Roozbahani, M., Khodadadi, M., 2021. Determination of total petroleum hydrocarbons and selected heavy metal (Pb, CO, V, Ni) concentration levels in surficial sediments of the Arvand River Estuary and their impact on benthic macroinvertebrates assemblages. *Int. J. Environ. Anal. Chem.* 1–17.
- Rahman, A., Sarkar, A., Yadav, O.P., Achari, G., Slobodnik, J., 2021. Potential human health risks due to environmental exposure to nano-and microplastics and knowledge gaps: A scoping review. *Sci. Total Environ.* 757, 143872.
- Rochman, C.M., 2018. Microplastics research—from sink to source. *Science (80-.)*. 360, 28–29.
- Rodrigues, M.O., Abrantes, N., Gonçalves, F.J.M., Nogueira, H., Marques, J.C., Gonçalves,

- A.M.M., 2018. Spatial and temporal distribution of microplastics in water and sediments of a freshwater system (Antuã River, Portugal). *Sci. Total Environ.* 633, 1549–1559.
- Ryan, J., Estefan, G., Rashid, A., 2001. Soil and plant analysis laboratory manual. ICARDA.
- Sagawa, N., Kawaai, K., Hinata, H., 2018. Abundance and size of microplastics in a coastal sea: comparison among bottom sediment, beach sediment, and surface water. *Mar. Pollut. Bull.* 133, 532–542.
- Sam, S.T., Nuradibah, M.A., Ismail, H., Noriman, N.Z., Ragunathan, S., 2014. Recent advances in polyolefins/natural polymer blends used for packaging application. *Polym. Plast. Technol. Eng.* 53, 631–644.
- Savoca, M.S., Wohlfeil, M.E., Ebeler, S.E., Nevitt, G.A., 2016. Marine plastic debris emits a keystone infochemical for olfactory foraging seabirds 1–9.
- Scherer, C., Weber, A., Stock, F., Vurusic, S., Egerci, H., Kochleus, C., Arendt, N., Foeldi, C., Dierkes, G., Wagner, M., 2020. Comparative assessment of microplastics in water and sediment of a large European river. *Sci. Total Environ.* 738, 139866.
- Sekudewicz, I., Dąbrowska, A.M., Syczewski, M.D., 2021. Microplastic pollution in surface water and sediments in the urban section of the Vistula River (Poland). *Sci. Total Environ.* 762, 143111.
- Severini, M.D.F., Buzzi, N.S., López, A.D.F., Colombo, C.V., Sartor, G.L.C., Rimondino, G.N., Truchet, D.M., 2020. Chemical composition and abundance of microplastics in the muscle of commercial shrimp *Pleoticus muelleri* at an impacted coastal environment (Southwestern Atlantic). *Mar. Pollut. Bull.* 161, 111700.
- Shruti, V.C., Jonathan, M.P., Rodriguez-Espinosa, P.F., Rodríguez-González, F., 2019. Microplastics in freshwater sediments of atoyac river basin, puebla city, Mexico. *Sci. Total Environ.* 708, 136077.

- Environ. 654, 154–163.
- Simon, M., Hartmann, N.B., Vollertsen, J., 2021. Accelerated Weathering Increases the Release of Toxic Leachates from Microplastic Particles as Demonstrated through Altered Toxicity to the Green Algae *Raphidocelis subcapitata*. *Toxics* 9, 185.
- Sissakian, V., Abdul Ahad, A., Al-Ansari, N., Knutsson, S., 2017. Geomorphology, geology and tectonics of Jabal Sanam, southern Iraq. *J. Earth Sci. Geotech. Eng.* 7, 97–113.
- Song, Y.K., Hong, S.H., Jang, M., Han, G.M., Jung, S.W., Shim, W.J., 2017. Combined effects of UV exposure duration and mechanical abrasion on microplastic fragmentation by polymer type. *Environ. Sci. Technol.* 51, 4368–4376.
- Stolte, A., Forster, S., Gerds, G., Schubert, H., 2015. Microplastic concentrations in beach sediments along the German Baltic coast. *Mar. Pollut. Bull.* 99, 216–229.
- Strokal, M., Bai, Z., Franssen, W., Hołtrą, N., Koelmans, A.A., Ludwig, F., Ma, L., van Puijenbroek, P., Spanier, J.E., Vermeulen, L.C., 2021. Urbanization: an increasing source of multiple pollutants to rivers in the 21st century. *npj Urban Sustain.* 1, 1–13.
- Tibbetts, J., Krause, S., Lynch, I., Sambrook Smith, G.H., 2018. Abundance, distribution, and drivers of microplastic contamination in urban river environments. *Water* 10, 1597.
- Uheida, A., Mejía, H.G., Abdel-Rehim, M., Hamd, W., Dutta, J., 2021. Visible light photocatalytic degradation of polypropylene microplastics in a continuous water flow system. *J. Hazard. Mater.* 406, 124299.
- van Emmerik, T., Schwarz, A., 2020. Plastic debris in rivers. *Wiley Interdiscip. Rev. Water* 7, e1398.
- Wagner, J., Wang, Z.-M., Ghosal, S., Rochman, C., Gassel, M., Wall, S., 2017. Novel method for the extraction and identification of microplastics in ocean trawl and fish gut matrices.

- Anal. Methods 9, 1479–1490.
- Wagner, S., Klöckner, P., Stier, B., Römer, M., Seiwert, B., Reemtsma, T., Schmidt, C., 2019. Relationship between discharge and river plastic concentrations in a rural and an urban catchment. *Environ. Sci. Technol.* 53, 10082–10091.
- Wang, F., Wang, B., Duan, L., Zhang, Y., Zhou, Y., Sui, Q., Xu, D., Qu, H., Yu, G., 2020. Occurrence and distribution of microplastics in domestic, industrial, agricultural and aquacultural wastewater sources: A case study in Changzhou, China. *Water Res.* 182, 115956.
- Wang, J., Peng, J., Tan, Z., Gao, Y., Zhan, Z., Chen, Q., Cai, L., 2017. Microplastics in the surface sediments from the Beijiang River littoral zone: composition, abundance, surface textures and interaction with heavy metals. *Chemosphere* 171, 248–258.
- Wang, J., Tan, Z., Peng, J., Qiu, Q., Li, M., 2016. The behaviors of microplastics in the marine environment. *Mar. Environ. Res.* 113, 7–17.
- Wang, J., Wang, M., Ru, S., Liu, X., 2019. High levels of microplastic pollution in the sediments and benthic organisms of the South Yellow Sea, China. *Sci. Total Environ.* 651, 1661–1669.
- Wang, Z., An, C., Chen, X., Lee, K., Zhang, B., Feng, Q., 2021. Disposable masks release microplastics to the aqueous environment with exacerbation by natural weathering. *J. Hazard. Mater.* 417, 126036.
- Xu, P., Peng, G., Su, L., Gao, Y., Gao, L., Li, D., 2018. Microplastic risk assessment in surface waters: A case study in the Changjiang Estuary, China. *Mar. Pollut. Bull.* 133, 647–654.
- Yan, M., Nie, H., Xu, K., He, Y., Hu, Y., Huang, Y., Wang, J., 2019. Microplastic abundance, distribution and composition in the Pearl River along Guangzhou city and Pearl River

- estuary, China. *Chemosphere* 217, 879–886.
- Yang, L., Zhang, Y., Kang, S., Wang, Z., Wu, C., 2021. Microplastics in soil: A review on methods, occurrence, sources, and potential risk. *Sci. Total Environ.* 146546.
- Yu, Y., Mo, W.Y., Luukkonen, T., 2021. Adsorption behaviour and interaction of organic micropollutants with nano and microplastics—A review. *Sci. Total Environ.* 149140.
- Zhang, K., Gong, W., Lv, J., Xiong, X., Wu, C., 2015. Accumulation of floating microplastics behind the Three Gorges Dam. *Environ. Pollut.* 204, 117–123.
- Zhao, S., Zhu, L., Li, D., 2015. Microplastic in three urban estuaries, China. *Environ. Pollut.* 206, 597–604.
- Zhou, Q., Zhang, H., Fu, C., Zhou, Y., Dai, Z., Li, Y., Fu, C., Luo, Y., 2018. The distribution and morphology of microplastics in coastal soils adjacent to the Bohai Sea and the Yellow Sea. *Geoderma* 322, 201–208.

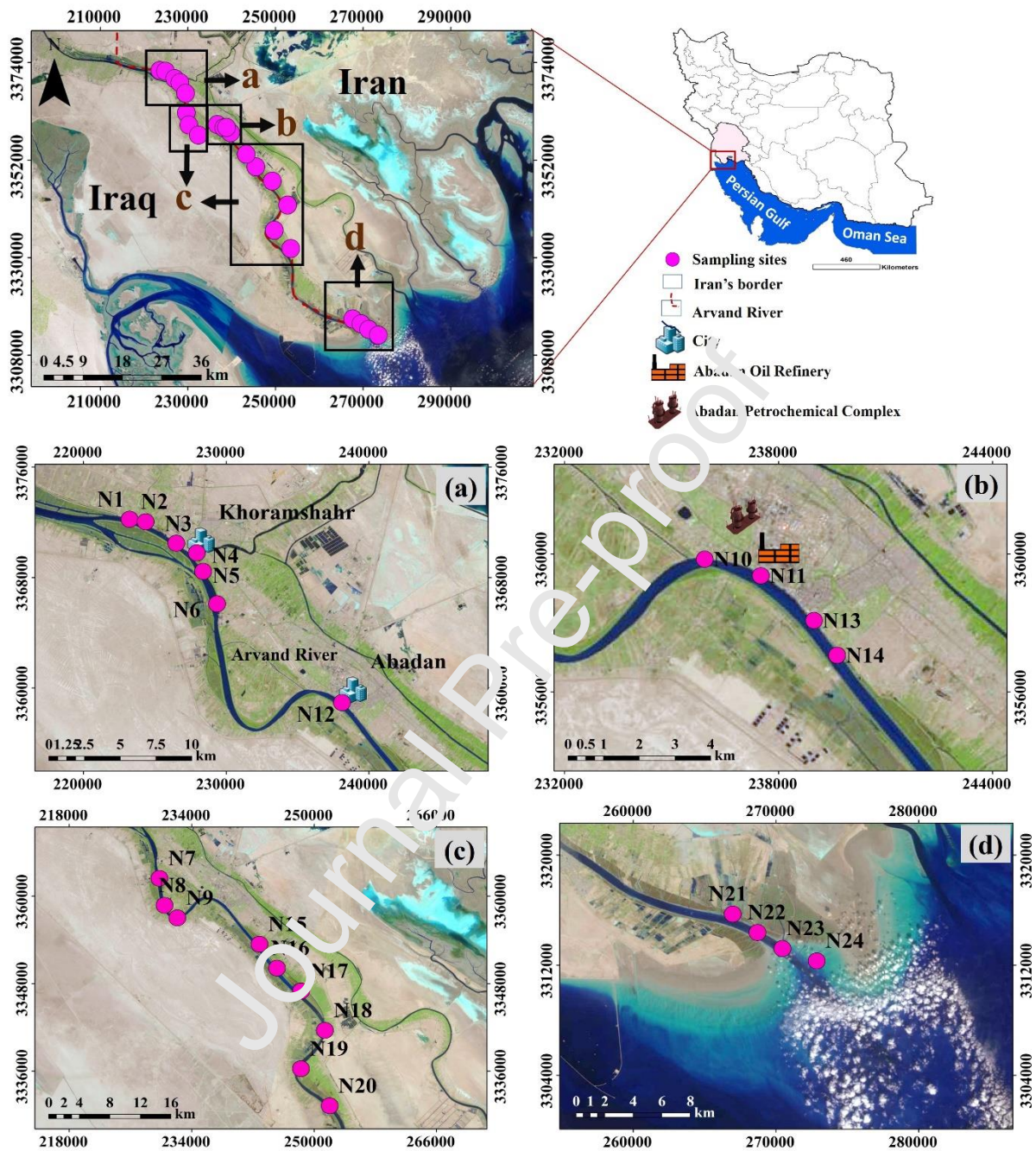


Fig. 1. Sampling locations of surface water and sediment in different land uses: (a) urban; (b) industrial; (c) agricultural; and (d) natural areas of the Arvand River, Persian Gulf. Background image (Landsat 8 OLI/TIRS C1 Level-2) is obtained from earthexplorer.usgs.gov.

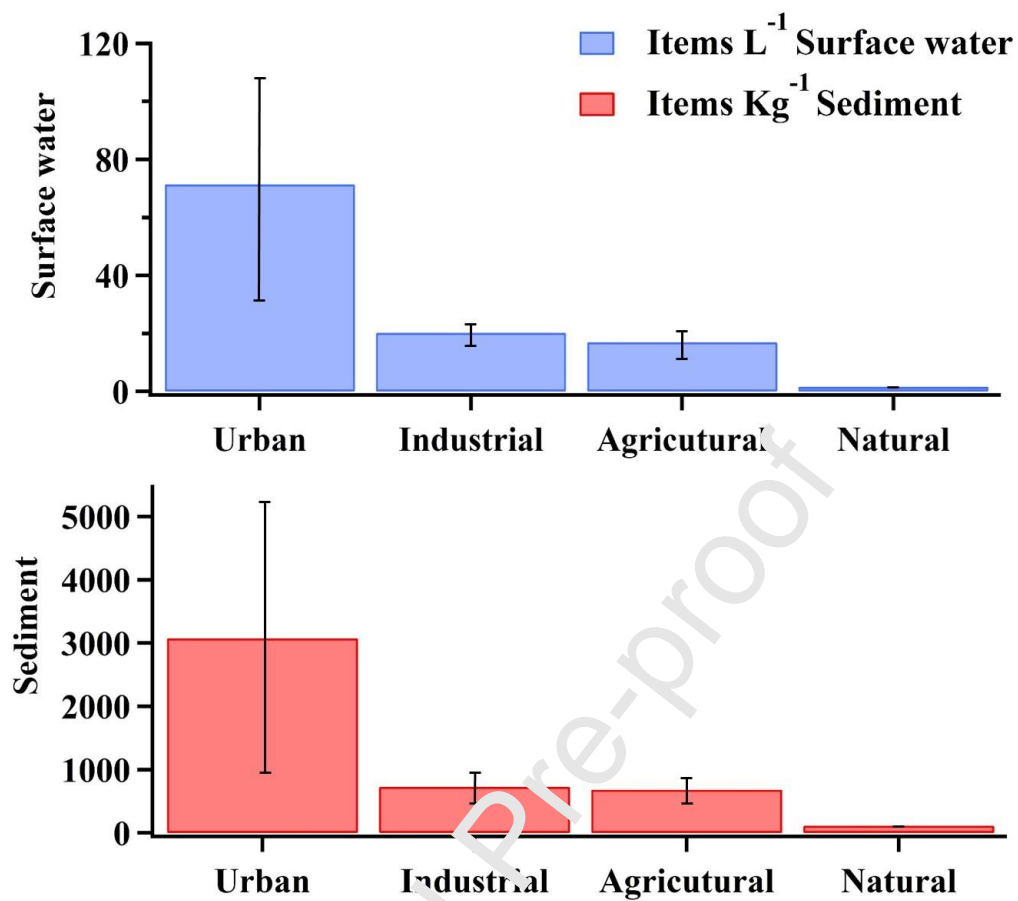


Fig. 2. Mean abundance of MPs (mean + error bar) in surface water and sediment collected from different land uses along the Arvand River.

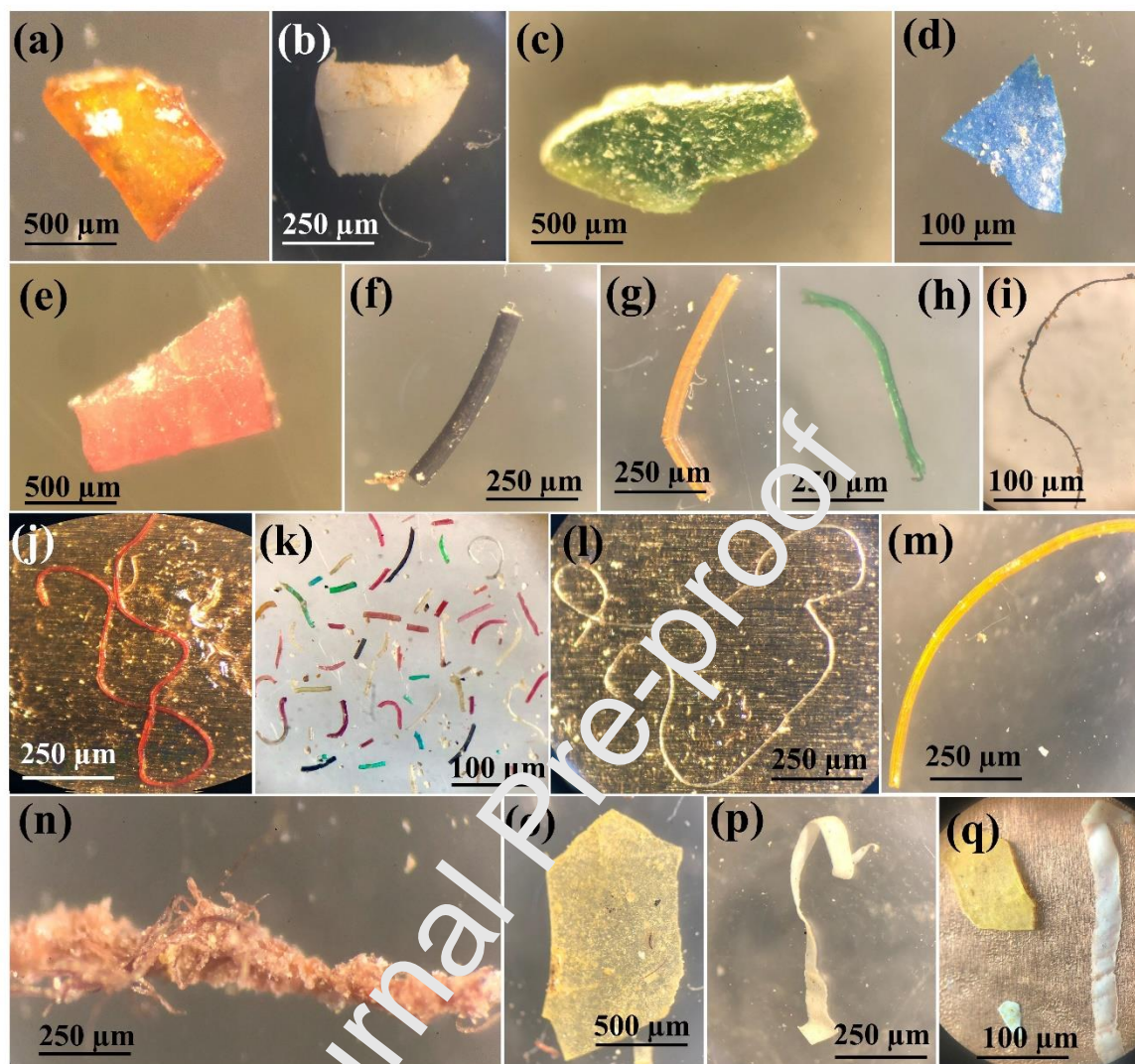


Fig. 3. MPs extracted from sediment and water from the Arvand River. The images were taken with a binocular optical microscope (Carl-Zeiss, Oberkochen/West Germany). a–e: Fragments, f–m: fibers, n: tangled fibers, o–q: films.

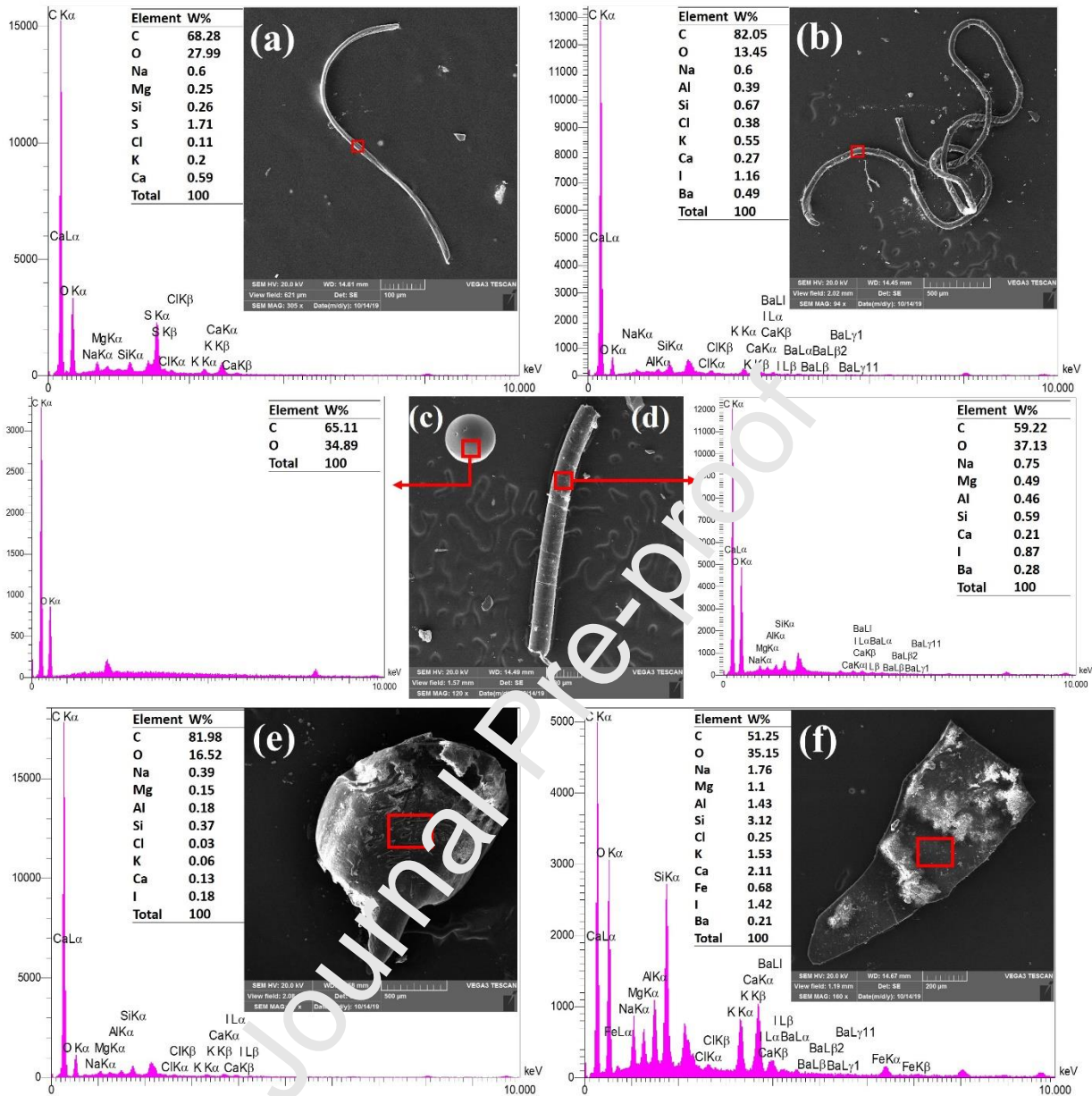


Fig. 4. SEM images and EDX of representative MPs found in the Arvand River including: (a) fiber particle separated from water sample; (b) long fiber MPs extracted from sediment sample in urban area; (c) spherule found in sediment sample of urban area; (d) line/fiber MPs in sediment sample of urban area; (e) fragment MPs extracted from sediment sample of agricultural sector; and (f) film particle in water sample of urban area.

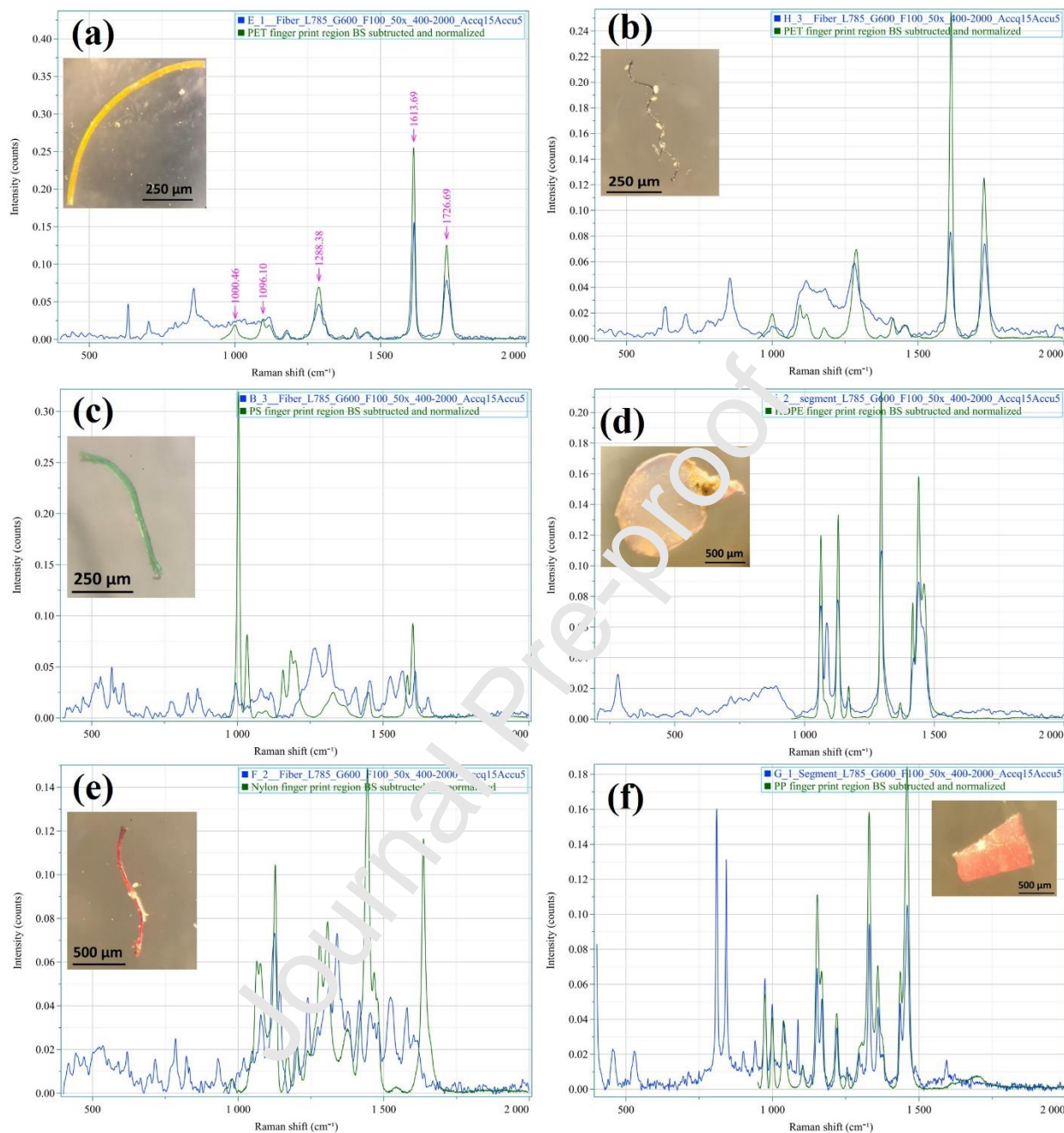


Fig. 5. Raman spectra of some MPs found in surface water and sediment: (a) yellow fiber, polyethylene terephthalates (PET); (b) black fiber, PET, (c) green fiber, polystyrene (PS); (d) transparent fragment, high density polyethylene (HDPE); (e) red fiber, nylon; and (f) red fragment, polypropylene (PP).

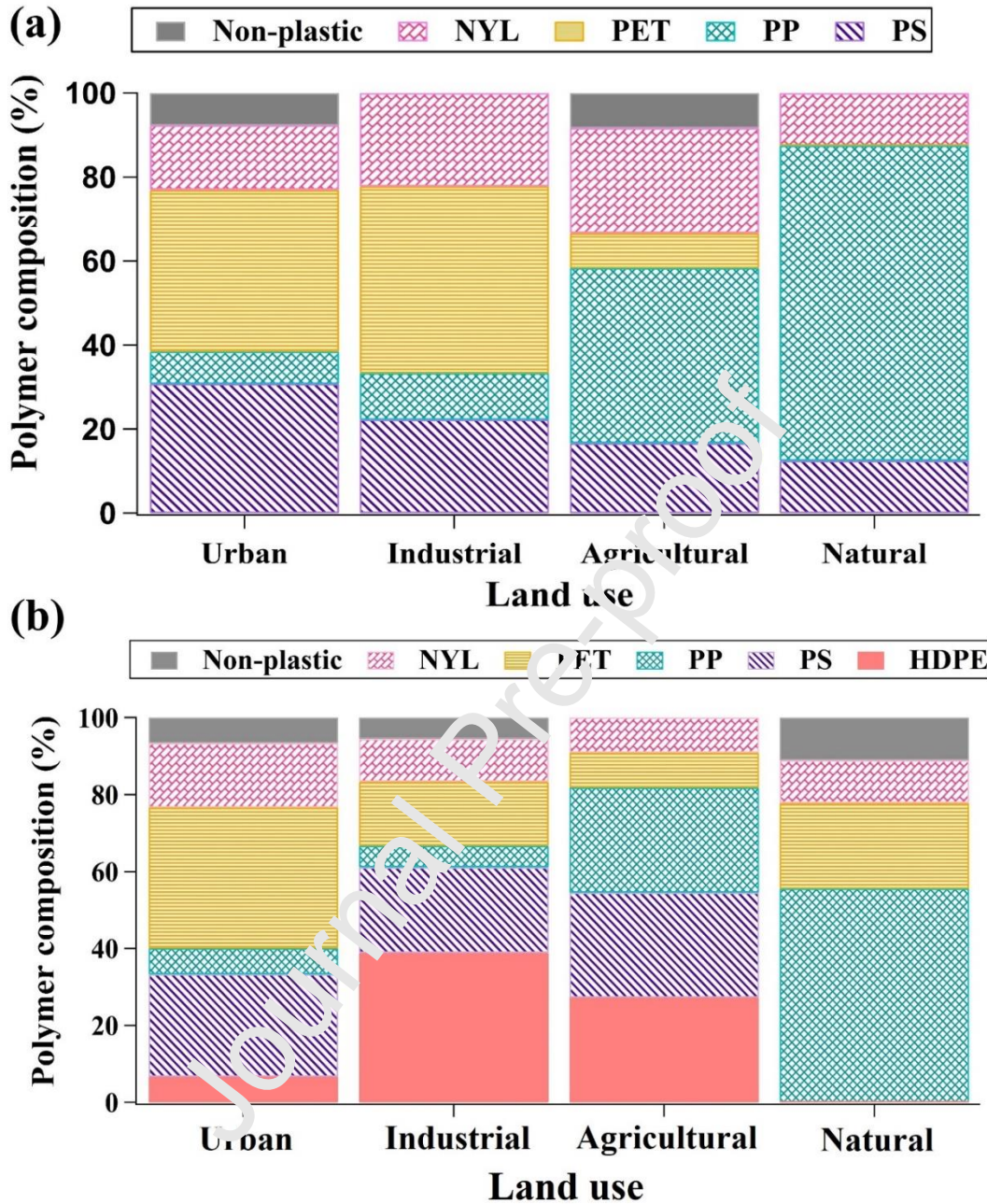


Fig 6. Polymer compositions in (a) surface water and (b) surface sediment from the different land uses across the Arvand River.

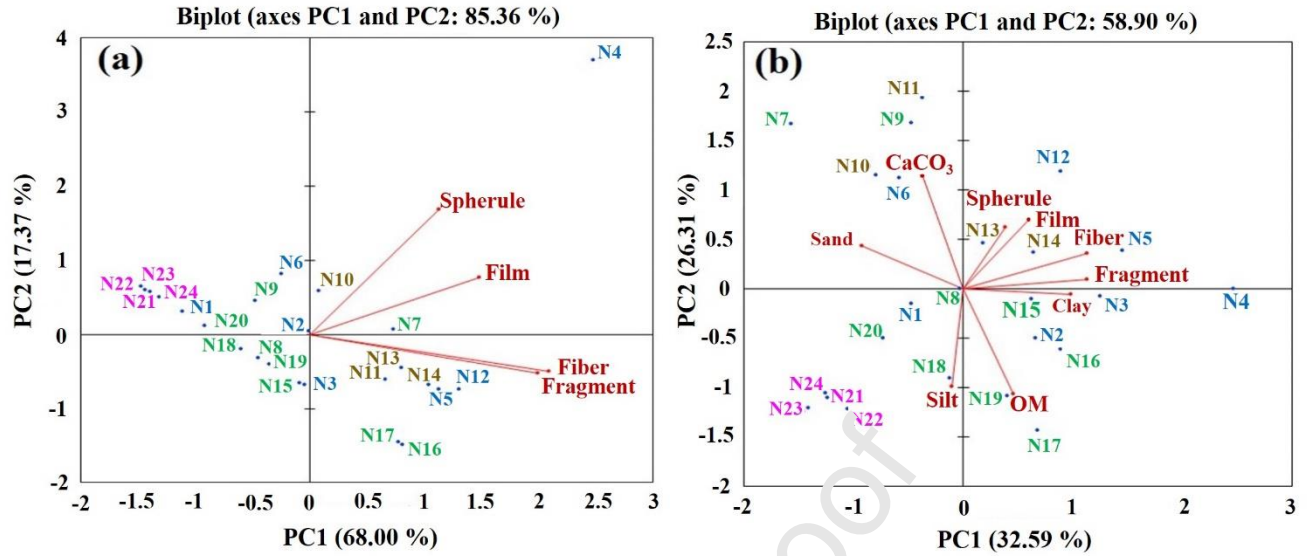


Fig 7. PCA biplot showing interrelations of different types of MPs in (a) water and (b) sediment sampling sites. Samples collected from the urban, agricultural, industrial and natural land uses are distinguished by blue, green, brown, and pink colors, respectively.

Table 1. p-values obtained from the independent t-test and one-way ANOVA with normalized MP concentrations in water and sediment in different land uses.

Statistical test	Constant Variable	P-value	
		Water	Sediment
Independent t-test	Water & sediment	0	0
Levene Statistic test		0.657	0.657
One-way ANOVA test			
Levene Statistic test		0.003	0.019
Welch test		0	0.001
Brown-Forsythe		0.003	0.032
ANOVA Between Groups	Land-use	0.002	0.036
Dunnnett T3 test			
Urban	Agricultural	0.835	0.961
	Industrial	0.994	0.997
	Natural	0.014	0.078
Agricultural	Urban	0.835	0.961
	Industrial	0.791	0.991
	Natural	0	0.002
Industrial	Urban	0.994	0.997
	Agricultural	0.791	0.991
	Natural	0.001	0.011
Natural	Urban	0.014	0.078
	Agricultural	0	0.002
	Industrial	0.001	0.011

CRedit authorship contribution statement

Naghmeh Soltani: Conceptualization, Investigation, Writing - original draft. **Behnam Keshavarzi:** Supervision, Validation, Resources. **Farid Moore:** Supervision, Review & editing, Resources. **Rosa Busquets:** Review & editing. **Mohammad Javad Nematollahi:** Writing, Formal analysis. **Sylvie Gobert:** Review & editing. **Reza Javid:** Investigation, Logistical supporting. All authors discussed the results and contributed to the final manuscript.

Journal Pre-proof

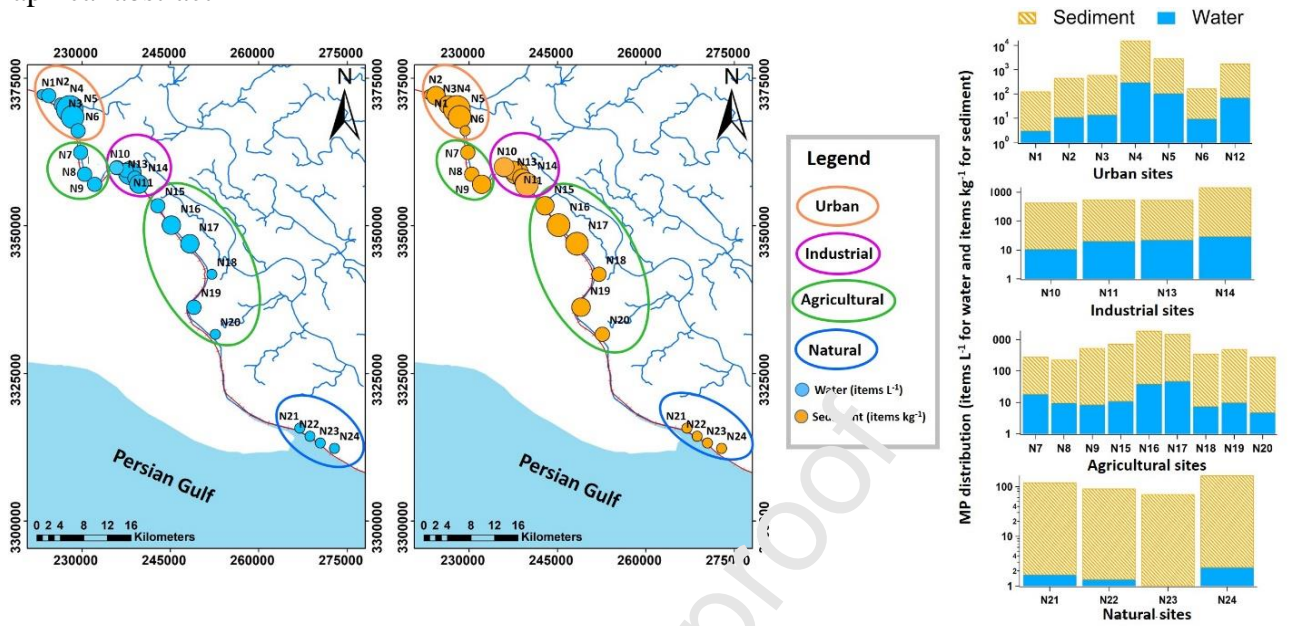
Declaration of interests

The authors declare that they have no known competing financial interests or personal relationships that could have appeared to influence the work reported in this paper.

The authors declare the following financial interests/personal relationships which may be considered as potential competing interests:

Journal Pre-proof

Graphical abstract



Highlights

- The first microplastic (MP) assessment in water/ sediments of the Arvand River.
- MP contamination was greater in urban than in industrial/agricultural/ natural areas.
- Fibres; 200-500 and >1000 μm MPs; PET/PP (water), PET/ PS (sediment) dominated.
- Urban effluents behind MP hotspots in water and sediment.
- Clay and organic matter can control MPs distribution in sediment

Journal Pre-proof